Research on the Forecasting and Risk Analysis Method of Snowmelt Flood

Pengfei Zhou
Institute of Public Safety Research,
Department of Engineering Physics, Tsinghua University
zpf18@mails.tsinghua.edu.cn

Tao Chen
Institute of Public Safety Research,
Department of Engineering Physics, Tsinghua University
matthieu.lauras@mines-albi.fr

Guofeng Su
Institute of Public Safety Research,
Department of Engineering Physics, Tsinghua University
sugf@tsinghua.edu.cn

Bingxu Hou
Beijing Global Safety Technology Co. Ltd.
houbingxu@gsafety.com

Lida Huang
Institute of Public Safety Research, Department of Engineering Physics, Tsinghua University
huanglida@tsinghua.edu.cn

ABSTRACT

Risk analysis of snowmelt flood is an urgent demand in cold highland areas. This paper focuses on the method for the rapid and reliable forecast of daily snowmelt, snow water runoff, and snowmelt flood risk. A neural network algorithm is used to calculate snow density distribution, snow depth and snow-water equivalent with the brightness temperature data. Then, daily snowmelt is predicted using the degree-day factor method with the temperature distribution. On this basis, we use the steepest descent method and Manning formula with hydrographic information to simulate snow water runoff. We also propose a method to predict the snowmelt flood risk with the geographic feature and historical flood data. The evaluated risk is compared with monitored data in the Xinjiang Autonomous Region of China, which shows good consistency. At last, we develop a risk analysis system to generate the snowmelt flood risk map and provide risk analysis service.

Keywords

Snowmelt Flood, Daily Snowmelt, Snow Water Runoff, Risk Analysis, Forecasting Method.

INTRODUCTION

About 60% land area in the world is covered by seasonal snow, with 9×10^6 km^2 (Niu 2017). Due to the effects of climate change and global warming, the risk of snowmelt flood in spring is greatly increased, posing a serious threat to the safety of surrounding cities and towns. Every year, the snowmelt flood causes huge losses to the infrastructure, houses, and assets in the disaster area. Therefore, it is very necessary to study the forecasting method of snowmelt flood.

However, most of the snow-capped mountains are located in remote areas with complex mountainous terrain, which makes it difficult to obtain data on the spot. As a result, it is economical and feasible to use the remote sensing satellite to detect the snow data and predict the snowmelt volume by using the algorithm. Combined with local hydrological and geographical features, flood runoff is obtained to predict and warn the flood evolution area.

It is of great significance for snowmelt flood warning, water resource allocation in the basin, and urban disaster reduction.

Many scholars have researched the forecasting methods of snowmelt floods. In the research on the snow ablation rate, Deutscher and Osterreichischer (1900) found a linear relationship between snow ablation rate and snow surface temperature. Based on this discovery, the classical "degree-day" snowmelt model was constructed, which has been studied and improved by many researchers. By using the multiple regression, Lang (1968) added water vapor pressure and radiation variables in the model to improve the simulation accuracy. Marinec and Rango (1986) adjusted the degree factor and snow density according to the vegetation and plant coverage in the basin. Recently, some novel snowmelt flood forecasting models have been proposed. In 2004, the USM (Urban Snow Model) model was constructed based on energy balance, which combined snow surface reflectivity with different types of snow cover information (Valeo and Ho 2004). The simulation results showed that compared with the "degree-day" model, the USM model had a higher simulation accuracy in urban areas. In 2008, the SRM (Short-term Runoff Model) model based on remote sensing and meteorological data was used to predict short-term snowmelt runoff in the Alps (Thomas et al. 2008). In 2011, the SHETRAN model was used to analyze the impact of plant cover on floods caused by extreme snowfall and rainfall in four different small watersheds in the United States (Bathurst et al. 2011). In 2012, to simulate snowmelt runoff changes in the Cotton Creek, Jost et al. (2012) constructed a distributed temperature-index snowmelt model summarizing the advantages of several models like as the DHSVM (Wigmosta et al. 1994) and ISNOBAL (Link et al. 1999). In 2018, Shen et al. (2018) detected streamflow trends by Mann-Kendall tests and analyzed changes in snowmelt runoff timing based on the winter snowmelt runoff center time (WSCT) in the southern Tianshan Mountains.

The above studies laid the foundation for the snow water equivalent inversion and flood runoff simulation, but there are few studies on the integration and display of flood forecasting and risk analysis. In this paper, we construct a system including functions of snowmelt forecasting, flood runoff forecasting and flood risk forecasting. The evolution and distribution of snow floods in the region are predicted comprehensively and accurately, and then the flood evolution process is visualized by image and video. Our research provides a comprehensive solution for predicting flood evolution and risk distribution.

The remainder of this paper is structured as follows. Section 2 provides an overview of methods to realize the forecasting and risk analysis. Section 3 shows the schematic diagrams of snowmelt flood risk, daily snowmelt and flood evolution in the system. Section 4 shows the simulation results of daily snowmelt and flood risk in Ili and Section 5 makes a conclusion.

METHODS

Runoff Forecasting Method

Our runoff forecasting method is shown in Figure 1. This forecasting method includes 3 sections. Section 1 is a neural network algorithm used to retrieve the snow water equivalent (SWE). Section 2 is the degree-day number (NDD) algorithm used to obtain daily snowmelt (DSM). Section 3 is the runoff model used to obtain the flood runoff distribution.

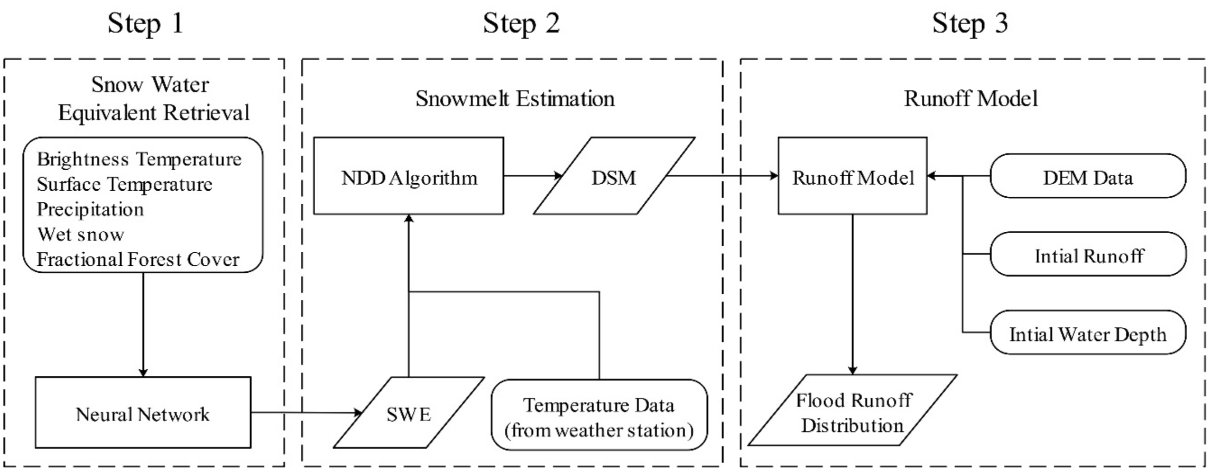

Figure 1. Flow chart of runoff forecasting.

Snow Water Equivalent Retrieval

Snow depth (SD) refers to the vertical depth from the surface of the snow layer to the ground below the snow, assuming the snow layer is evenly distributed over the snowy ground. Snow water equivalent (SWE) refers to the vertical depth of the water layer formed when the snow is completely melted. As the snow has different sensitivity to various frequencies, the 19GHz and 37GHz horizontal polarization brightness temperature data collected by Advanced Microwave Scanning Radiometer-EOS (AMSR-E) sensor is widely used to inverse SD and SWE by linear regression algorithm (Xiong and Guo 2004). The conversion between snow depth and snow water equivalent generally uses the following formula:

$$\mathrm{SWE} = SD \times \rho_{\mathrm{snow}} \tag{1}$$

Where SWE is snow water equivalent, SD is the snow depth, and ρsnow is the snow density.

Because snow water equivalent has a strong correlation with parameters such as brightness temperature, surface temperature and precipitation, it is common to use machine learning methods to predict snow water equivalent. Among them, neural network performs the best, because it is very suitable for nonlinear complex classification work. So in this paper, a neural network algorithm is used to get snow depth, snow density and snow water equivalent (Alfred TC Chang 2000). Polarization brightness temperature data at 19 GHz and 37 GHz is used as input to retrieve SD. Factors such as surface temperature, precipitation, wet snow and fractional forest cover are used as inputs to retrieve ρ_{snow}. Then the output is SWE.

Snowmelt Estimation

Because the weather stations are widely distributed, the exact temperature data cannot be obtained for each location, so the temperature data need to be interpolated to obtain the temperature distribution. In this paper, we use Inverse Distance Weighted (IDW) interpolation method (Wang et al. 2014) to accomplish two dimensional discrete temperature data gridding calculation. The interpolation formula is:

$$Z = \left(\sum_{i=1}^{n} \frac{Z_i}{d_i^m} \right) / \left(\sum_{i=1}^{n} \frac{1}{d_i^m} \right) \tag{2}$$

Where Z is the estimated temperature value of the point to be interpolated; Zi is the observation temperature value in the weather station i; di is the distance between the station i and the point to be interpolated; n is the total number of stations participating in the interpolation calculation; m is the weight coefficient. The larger m is the huger contribution the sampling point will have to the interpolation result.

In the troposphere, for every 1km increase in altitude, the temperature drops by 6~7°C (here we take 6.5 ℃). The improved formula for IDW is:

$$Z = \left(\sum_{i=1}^{n} \frac{Z_i + 6.5 \dfrac{h_i - h}{1\mathrm{km}}}{d_i^m} \right) / \left(\sum_{i=1}^{n} \frac{1}{d_i^m} \right) \tag{3}$$

We use the degree-day factor model, which is the most widely used method for estimating snowmelt, using snow cover information, daily average temperature and degree-day factor, to estimate the amount of snowmelt (Lv et al. 2018).

The degree-day number (NDD) represents the energy absorbed by the snow. It can be obtained by calculating the arithmetic mean in the case of the temperature distribution measured at a fixed daily cycle. In the calculation, if the temperature is negative, replace it with 0 °C.

$$NDD = \frac{\sum_{i=1}^{n} T_i}{n} \left(T_i \geq 0 \right) \tag{4}$$

Where n is the number of measurements per day; Ti is the temperature in station i.

The negative temperature value is replaced by 0 °C because the amount of heat required to change the snow temperature below 0 °C is very small compared to the latent heat (80 cal/g) required to melt snow above 0 °C.

The daily maximum temperature is Tmax and the minimum temperature is Tmin. Because the processes of Tmin to Tmax, and Tmax to Tmin are linear changes, the daily temperature is a "Tmin-Tmax-Tmin" isosceles triangle distribution. Then the degree-day number NDD can be calculated by:

$$NDD = \begin{cases} 0, & \text{if } T_{\max} < 0 \\ T_{\max}^2 / 2\left(T_{\max} - T_{\min}\right) & \text{if } T_{\min} < 0 < T_{\max} \\ \left(T_{\max} + T_{\min}\right)/2 & \text{if } T_{\min} > 0 \end{cases} \tag{5}$$

The amount of snow melt (SM) is directly proportional to the NDD (SM=α×NDD) α is the degree-day factor (DDF), $a = 1.1(\frac{\rho_S}{\rho_W})$ where ρ_S and ρ_W are the density of snow and water; the unit of a is cm/°C/d.

SD and SWE can be accessed from remote sensing institute. According to the conservation of mass, the snow per unit area is completely melted into water ($\rho_S S_D A = \rho_W S_{we} A$).

Then there is $\frac{\rho_S}{\rho_W} = \frac{S_{we}}{S_D}$.

Using the degree-day factor method, the amount of daily snowmelt SM can be calculated from the snow cover density. If the calculated daily snowmelt DSM of a certain location exceeds the actual snow water equivalent of the location, the actual daily snowmelt amount needs to be corrected:

$$DSM = \begin{cases} SM \times 1d, & if\ SM \times 1d < S_{we} \\ Swe, & if\ SM \times 1d < S_{we} \end{cases} \tag{6}$$

Runoff Model

In terms of architecture, many of the humanitarian agencies are organized as federations or pools. Even within the group, organizations policies, structure and Runoff model includes flow direction matrix, flow rate matrix and hydrology model. The flow direction matrix determines the flow direction. The flow rate matrix determines the flow rate. The hydrology model considers the impact of the local hydrology characteristics on the runoff.

Flow Direction Matrix

Since water always flows to the lowest place, the steepest direction can be considered as the direction of water flow. So the steepest slope method is used to determine the direction of the water flow, which is represented by the D8 encoding method, the most suitable encoding rule for the steepest slope method (Fang et al. 2008). Figure 2 shows the code of D8 encoding method summarizing the water flow direction.

32	64	128
16	(i, j)	1
8	4	2

Figure 2. Code of D8 encoding method summarizing the water flow direction.

Based on the D8 algorithm, the DEM raster data are scanned one by one with a 3*3 matrix. Then the grid with the largest slope between the center grid and each adjacent grid is regarded as the outflow grid of the center grid.

If the grid is at the boundary, the direction points to the boundary, and it will remain unchanged in subsequent processing.

If the grid is not at the boundary, the slope algorithm between the processed grid and the adjacent 8 grids is:

$$S = \frac{D_Z}{D_i} \quad (7)$$

Where S is the slope between the two grids; D_i is the distance between the centers of the two grids (Denote the side length of the grid in the DEM data as d_{DEM}, D_i is equal to d_{DEM} when grids are adjacent or $\sqrt{2}d_{DEM}$ when grids are diagonal); D_Z is the elevation difference Δh between the two grid, and the grid elevation h is the sum of the grid DEM elevation h_{DEM} and the grid water depth h_W.

If the maximum slope value is less than or equal to 0, the grid is depression or flat, and -2 is assigned, indicating that the direction of the water flow is undetermined. If the maximum slope value is greater than 0 and the maximum value is only one, then this direction is the direction of the water flow of the grid. If the slope value is greater than 0 and there is more than one maximum value, it means there are complex grids having the same elevation. The grid with the lowest number is selected as the water flow direction.

Flow Rate Matrix

For non-river areas, the source of the kinetic energy of the water flow is mainly the difference between the conversion of gravitational potential energy and the loss of ground resistance. There the kinetic energy is related to the ground vegetation, roughness condition, slope, flow path, and so on. Here the Manning formula (Manning et al. 1890) is widely used in practical engineering to calculate the flow rate. The kinetic energy before the start of precipitation is set to 0, and the water depth is set to 0. The formula for calculating the flow rate is:

$$V = \frac{1}{n} \times R_h^{2/3} \times S^{1/2} \quad (8)$$

Where V is the flow rate on the slope surface; S is the slope; n is the roughness, which is a coefficient that comprehensively reflects the influence of the roughness of the pipe's wall surface on the water flow, and here is set to 0.3; R_h is the hydraulic radius, which is the ratio of the cross-sectional area of the fluid to the wet perimeter. The wet perimeter refers to the circumference of the fluid in contact with the open area of the open channel, excluding the perimeter portion that is in contact with the air. In practice, the size of the aspect ratio is often not noticed, and the hydraulic radius R_h is replaced by the average water depth H of the section.

Flow Quantity Calculation

For a grid, if its current flow rate is V, the fluence rate q flowing out of the grid at this moment is:

$$q = A \times V \quad (9)$$

Where A is the interface area of water flowing out of the grid, the size of which is equal to the product of the grid size and the current water depth ($A = \alpha \times h_w$).

Then, if the time step is dt, the amount of water flowing out of the grid in one time step is:

$$Q = q \times dt \quad (10)$$

The amount of water in the grid at the beginning of the time step is:

$$Q_0 = \alpha^2 \times h_w \quad (11)$$

Then the amount of water in the grid at the end of the time step is:

$$Q_1 = Q_0 - Q \quad (12)$$

Similarly, the downstream grid has a water increment of Q in this time step.

Hydrology Model

DEM data only reflects surface elevation, but does not contain hydrological information. If runoff calculation is based only on DEM data, the influence of surface initial water depth and river flow on surface water transport is neglected, and the resulting water depth distribution is unreasonable.

In order to obtain more reliable simulation results, we propose a model that adding hydrological models such as rivers, lakes and reservoirs to the Manning formula. So that the impact of the above hydrological characteristics on surface flood transport is considered in the initial water depth, flow direction and flow rate.

For the initial water depth, the initial water depth matrix of rivers, lakes and reservoirs is set separately. The initial water depth of lakes and reservoirs is set according to actual data. The water depth of each section of the river can be obtained by interpolation according to the data of the monitoring station.

For the flow direction, the initial flow of rivers, lakes and reservoirs is consistent with the runoff direction, and is determined according to the river vector data and the end point of the river curve as needed.

For the flow rate, it is determined based on the actual hydrological data. The lake flow rate is consistent with the surface runoff flow rate. The gate of reservoir is set to be open or closed. The reservoir is considered a lake when the gate is open. In the closed state, the reservoir is isolated from the outside world, and the flow velocity of the reservoir is 0.

Flood Risk Forecasting Method

Taking Xinjiang as an example, this section proposes a method for snowmelt flood risk prediction. Through literature investigation and analysis of spring snowmelt flood cases in Xinjiang, it is found that the main influence factors of spring snowmelt floods in northern Xinjiang are winter precipitation and spring temperature characteristics (Tian et al. 2011). Yan et al. (2009) consider winter precipitation factors and temperature factors, and models the risk of snowmelt flooding in northern Xinjiang from March to May.

The cumulative precipitation number and integrated temperature are easily available meteorological data. Combined with the local risk threshold, the fusion model is effective in predicting the flood risk level.

Cumulative Precipitation Number

In our model, the cumulative precipitation number N is used to reflect the winter precipitation factor. First, read the number of precipitation (including snowfall and rainfall) N_{Feb} in February of each state and county. In March, count the number of precipitation N_{Spr} from March 1 to the current date.

$$N = N_{Feb} + N_{Spr} \tag{13}$$

Integral Temperature

This model uses the integral temperature T to reflect the temperature factor. The integral temperature is defined as: because the processes of t_{min} to t_{max}, and t_{max} to t_{min} are linear changes, the daily temperature is a "t_{min}-t_{max}-t_{min}" isosceles triangle distribution.

The snow melting occurs above 0 °C. Therefore, the integral temperature t is the integral of the daily temperature distribution curve above 0 °C, that is, the area enclosed by the temperature distribution curve above 0 °C. Let the daily time (the distance between two t_{min}) be 1, there are:

$$T = \begin{cases} 0, & \text{if } t_{\max} < 0 \\ t_{\max}^2 / 2\left(t_{\max} - t_{\min}\right) & \text{if } t_{\min} < 0 < t_{\max} \\ \left(t_{\max} + t_{\min}\right)/2 & \text{if } t_{\min} > 0 \end{cases} \tag{14}$$

Model Fusion

Based on the cumulative precipitation number N and the integral temperature T, the risk of spring snowmelt floods in various states and counties in northern Xinjiang was modeled. Based on the collected flood cases, thresholds N_{cri} and T_{cri} are set for N and T. On a certain day, N and T of a certain county can be obtained based on meteorological temperature data. then:

1. If $N < 1/2\ N_{cri}$ and $T = 0$, the flood risk level is none;
2. If $N < N_{cri}$ and $T < T_{cri}$, the flood risk level is low;
3. If $N > N_{cri}$ and $T < T_{cri}$, or $N < N_{cri}$ and $T > T_{cri}$, the flood risk level is medium;
4. If $N > N_{cri}$ and $T > T_{cri}$, the flood risk level is high;
5. If no flood occurs after the risk level has reached, the flood risk level remains high until a flood occurs.

Considering the differences in geomorphology and climate of various states and counties in Xinjiang, different thresholds N_{cri} and T_{cri} are set for each state and county. The thresholds N_{cri} and T_{cri} of the states and counties in northern Xinjiang are shown in Table 1.

Table 1. Threshold of snowmelt flood parameters in counties in northern Xinjiang

County	N_{cri}	T_{cri}
Ili	15	1
Changji	10	3
Bortala	5	5
Qoqek	10	4
Altay	10	2
Urumqi	10	1
Kumul	10	3

SYSTEM CONSTRUCTION

The snowmelt calculation algorithm, runoff calculation algorithm and the flood risk forecasting method are integrated into the same system, while the visualization module is added. A snowmelt flood risk forecasting system with different functional modules can be obtained. The system structure is shown in Figure 3. In this paper, the system has three functional modules, namely risk forecasting, remote sensing monitoring and flood evolution.

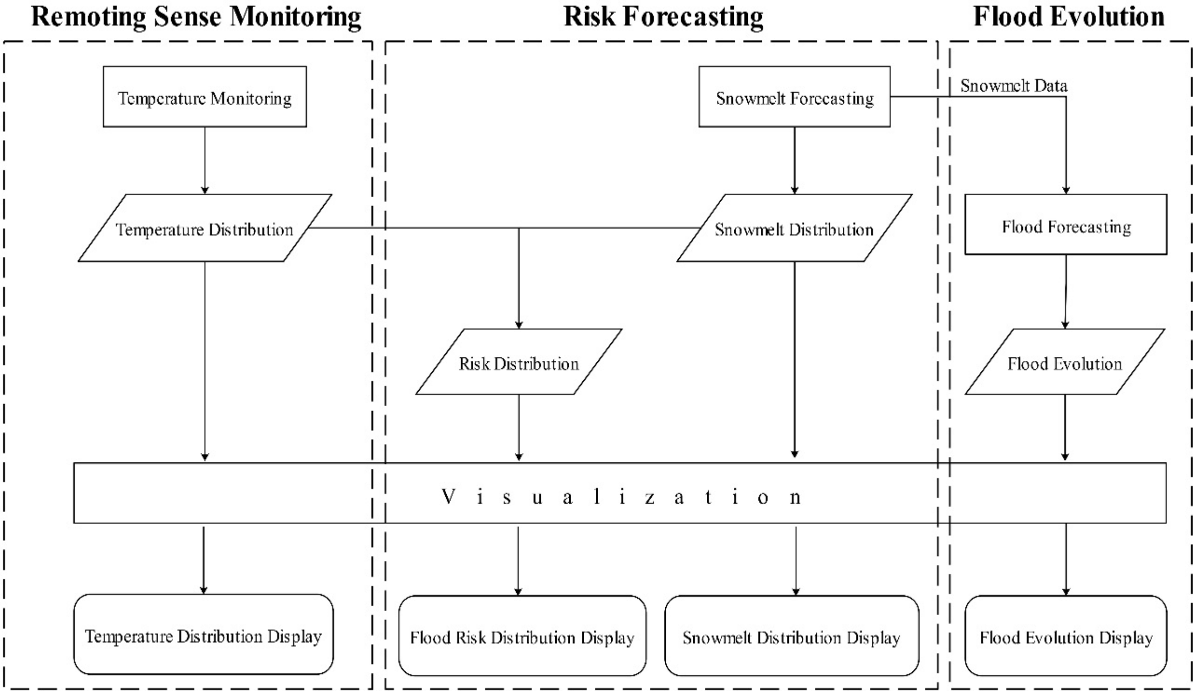

Figure 3. Flow chart of the system.

The flood risk forecasting function can realize the snowmelt flood risk forecasting in the whole region in the next 7 days. The forecasting diagram is shown in Figure 4. The figure shows the snow flood risk maps after 2 days, 3 days, 4 days and 6 days.

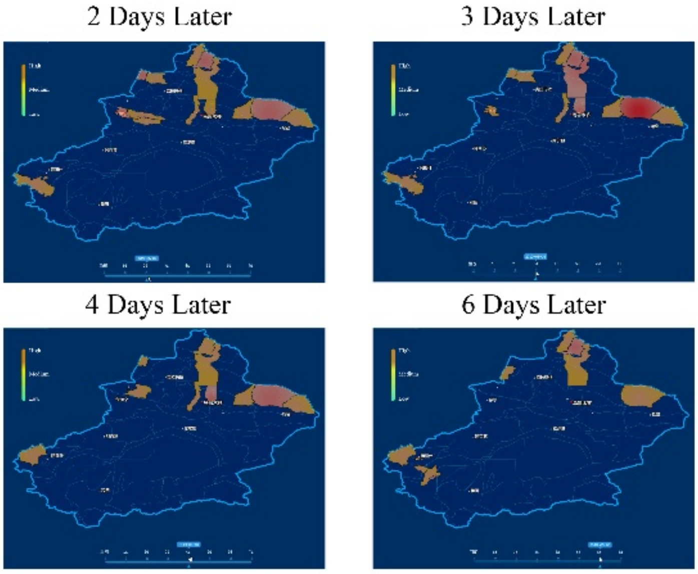

Figure 4. Schematic diagram of snowmelt flood risk in Xinjiang.

Based on the snowmelt calculation method, the snowmelt forecasting function can realize the real-time remote sensing data recording of the snowmelt in the past 30 days, and the forecasting of the snowmelt in the next three days. The snowmelt heat map of the corresponding date can be displayed by dragging the time axis. A schematic diagram of the recording and forecasting of the snowmelt data is shown in Figure 4.

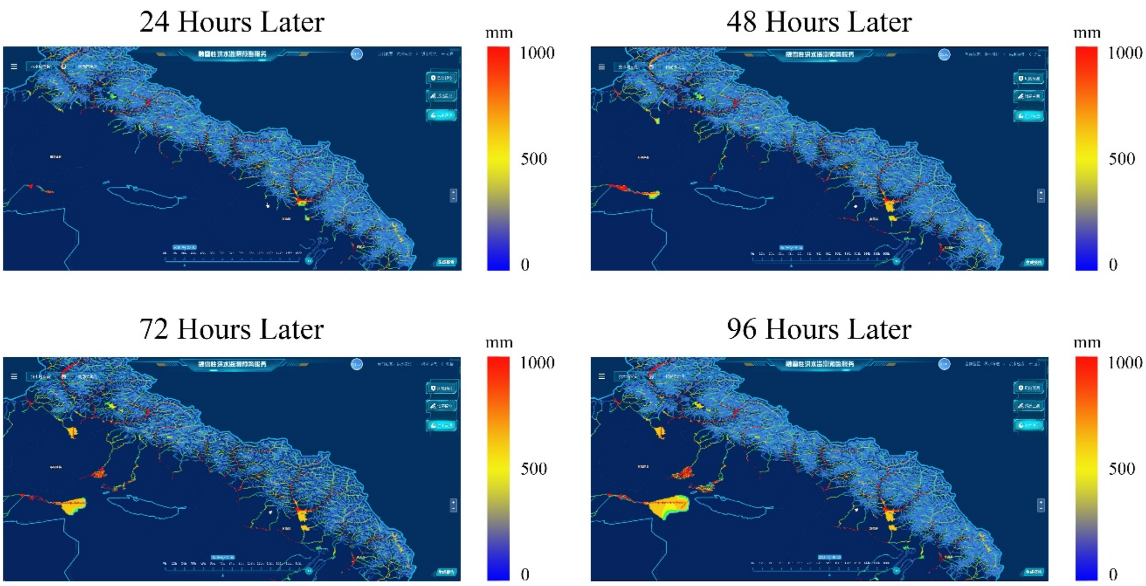

Figure 5. Schematic diagram of flood evolution in Xinjiang.

Based on the runoff calculation method, the dynamic demonstration of flood evolution in the next 7 days can be realized. The flood evolution trend is shown in Figure 5. The distribution of flood runoff within four days in the Altay region can be seen as follows.

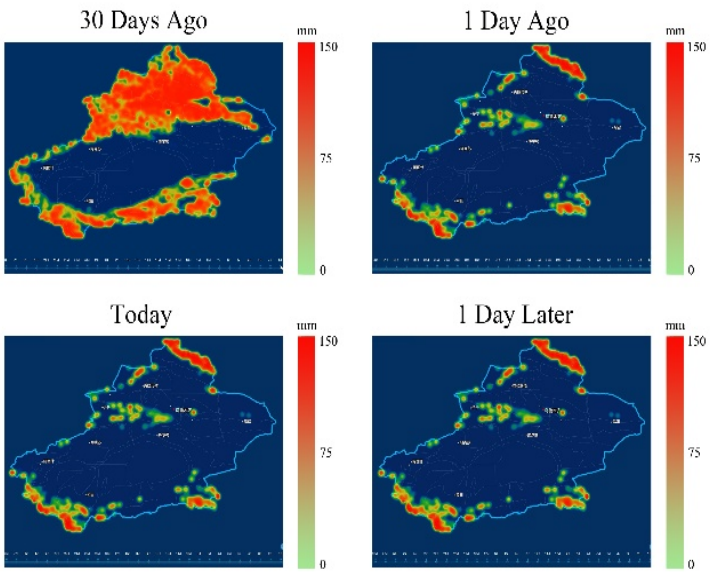

Figure 6. Schematic diagram of snowmelt in Xinjiang.

RESULTS

Daily Snowmelt of Ili

From the weather recording website, we collected the maximum and minimum temperature data of 9 counties in Ili from March 9 to 12, 2019.After getting these data, the daily snowmelt and snow water equivalent can be obtained according to the snowmelt calculation method. There are two situations.

Regardless of the elevation

The daily snowmelt (DSM) from March 9 to March 11 is shown in Figures 7 to 8.

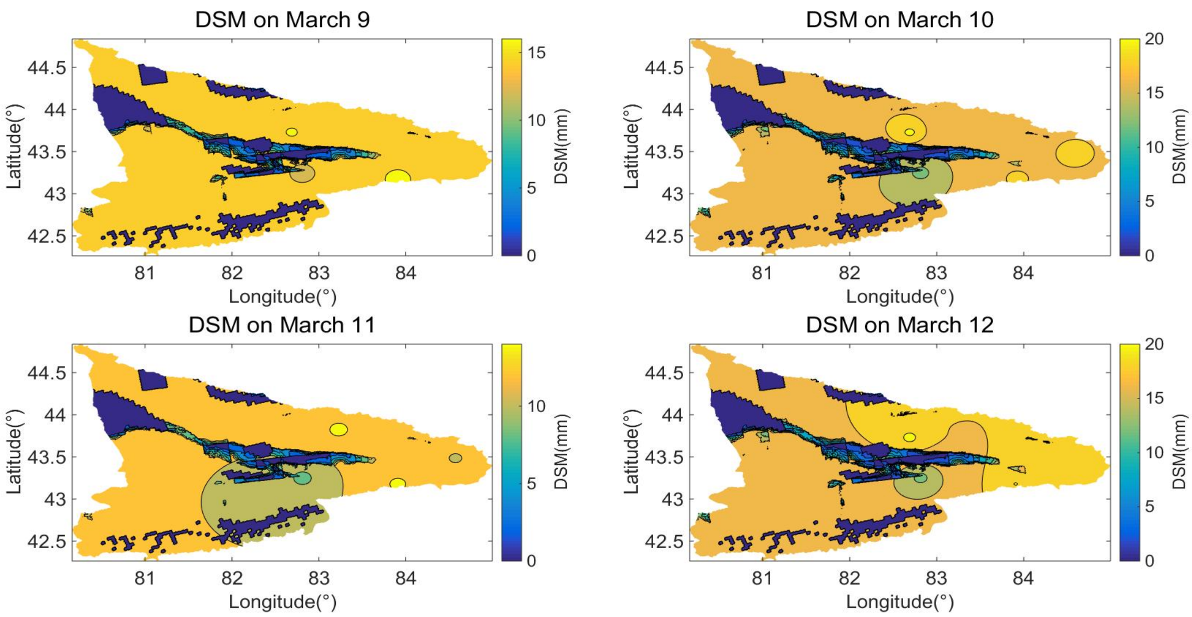

Figure 7. Calculated daily snowmelt (DSM) regardless of the elevation.

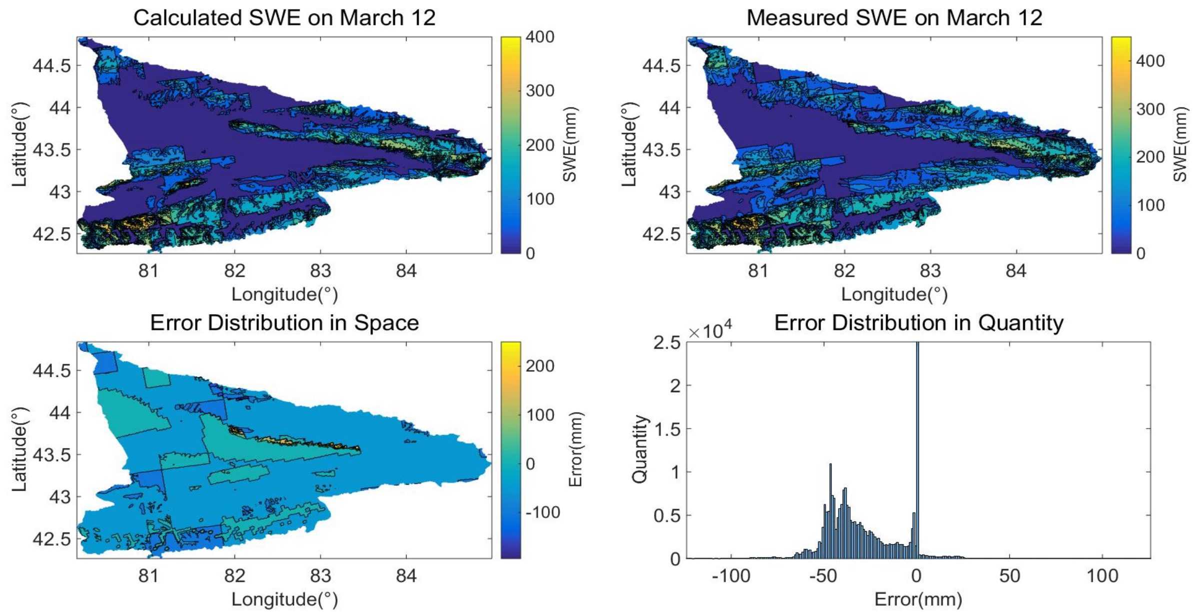

Figure 8. Calculated and Measured Snow Water Equivalent (SWE) regardless of the elevation, and error distribution between them.

According to the calculation, the error is mainly distributed between -50 and 0, the calculated mean is -25.94 mm, and the standard deviation is 26.98. The error we calculated is small with more simulated snowmelt.

Considering the elevation

The daily snowmelt (DSM) from March 9 to March 11 is shown in Figures 9 to 10.

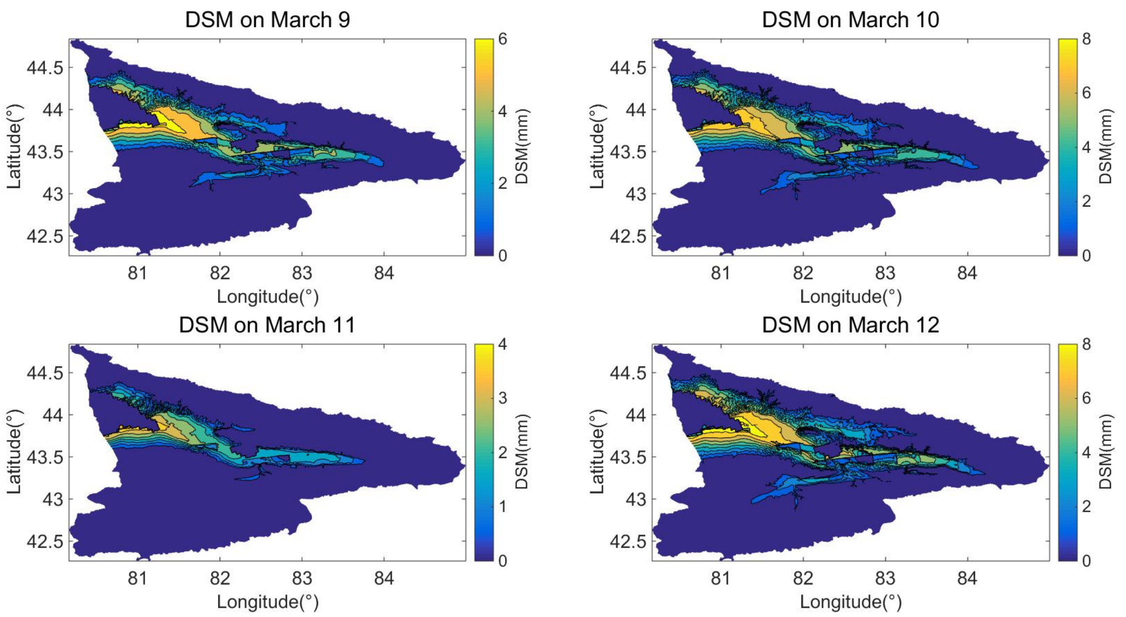

Figure 9. Calculated daily snowmelt (DSM) when considering the elevation.

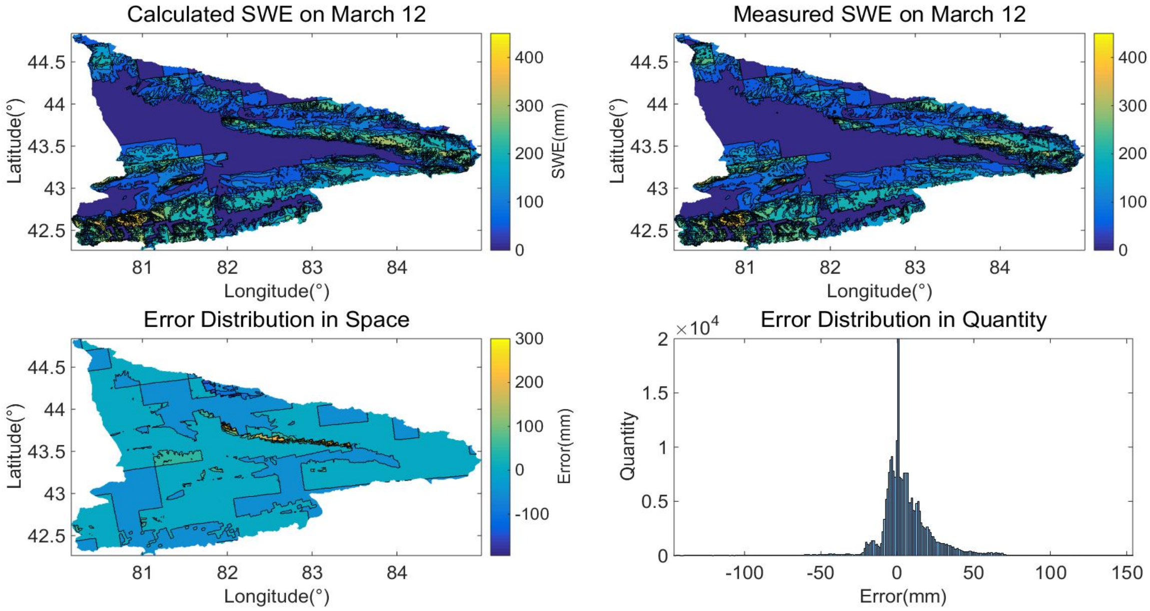

Figure 10. Calculated and Measured Snow Water Equivalent (SWE) regardless of the elevation, and error distribution between them.

According to the calculation, the error is mainly distributed between -25 and 50, the calculated mean is 6.54 mm, and the standard deviation is 24.89. The error we calculated is small with less simulated snowmelt.

Comparison of two situations

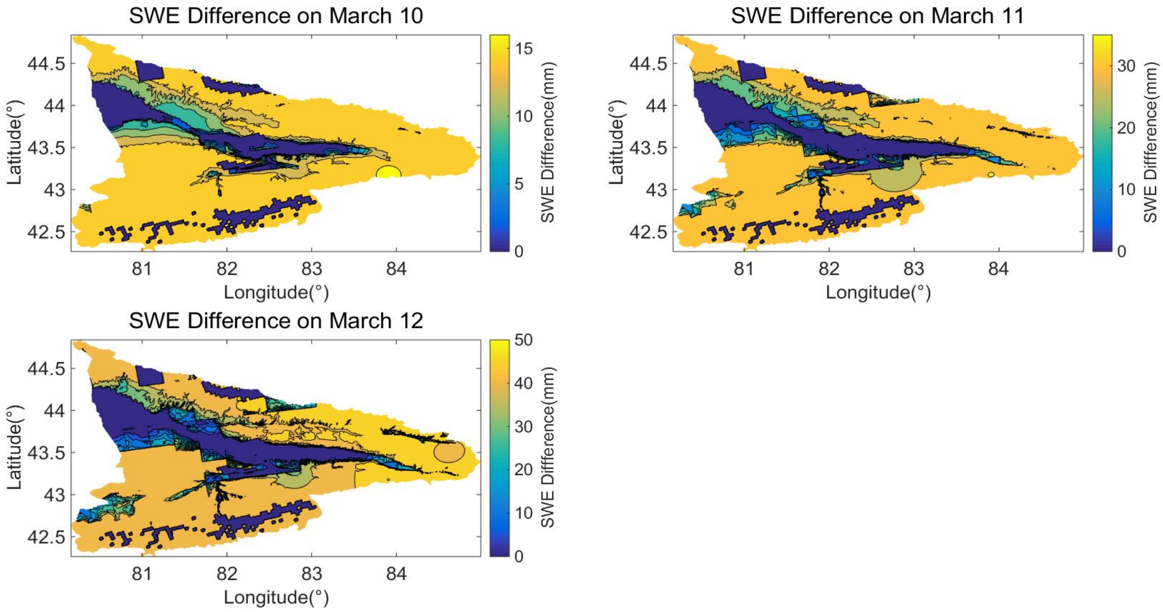

Figure 11. Snow water equivalent difference between two situations.

Data discussion: after the elevation data is considered, the corrections at high altitudes are obvious, but at the valleys are not obvious, as shown in the white part of Figure 11. This reduces errors and variances in both high altitude and valley locations. Therefore, increasing the elevation data can effectively reduce the calculation error and improve the running accuracy of the model. At the same time, observing the error map, it can be seen that the error with the measured value mainly distributes in the mountain range. Because the altitude of the mountain range changes greatly, resulting in the complex landform, and the uneven temperature distribution, which has an impact on the inversion of snowmelt.

Flood risk of Ili

Take the estimation of snowmelt flood risk in Ili on March 27, 2017 as an example. Table 2 lists the cumulative precipitation times N, the integral temperature T and the risk level of the counties in Ili on March, and the risk distribution is shown in Figure 12.

Table 2. Estimation of snowmelt flood risk in Ili on March 27, 2017

Name	N_{cri}	T_{cri}	Risk Level
Huocheng	23	7.5	High
Gulia	25	7.5	High
Nilka	27	4.5	High
Qapqal	24	7.5	High
Tokkuztara	28	7	High
Xinyuan	26	7	High
Zhaosu	28	2.5	Medium
Tekes	25	4.5	High

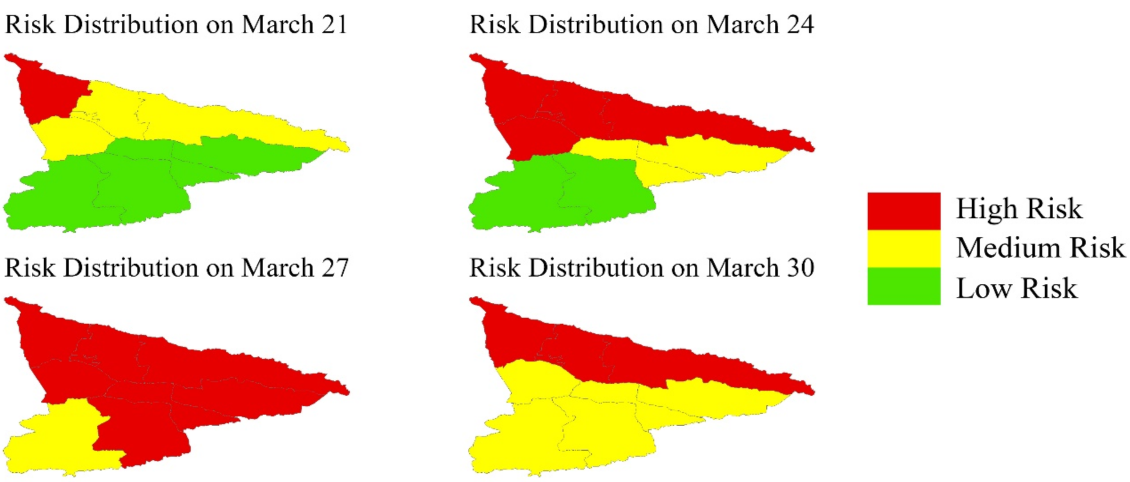

Figure 12. Risk distribution of snowmelt flood in Ili in March 2017.

CONCLUSION

In order to forecast the evolution of snowmelt flood, this paper uses the brightness temperature data detected by remote sensing satellites to inverse snow density distribution, snow depth and snow-water equivalent. Then, combing the snow water equivalent data with the local temperature distribution, the amount of daily snow is obtained. The snow water runoff and the distribution of flood evolution are forecasted with the daily snowmelt, local hydrological characteristics and geographical elevation characteristics. In addition, the paper uses historical flood data and climate characteristics to obtain flood risk distribution maps. Such results are compared with the historical case of a snow flood in Xinjiang, which shows good consistency. It turns out that our approach can realize the forecasting and risk analysis of snowmelt flood.

Although our forecasting results are basically in line with the actual snow flood distribution, the simulation accuracy still can be improved. Since the current input data is rough, if more accurate temperature data, hydrological data and basic geographic data are input in the future, it will be more exact in the forecasting of flood runoff and subdividing flood risk distribution.

Compared with other researchers only focusing on snow inversion or flood prediction, this paper integrates snowmelt estimation, runoff quantity and hydrology model to get a complete and structured system, which has a great supporting role for emergency decision. This system can be widely used for snowmelt flood prediction in high altitude and high latitude regions. The next step is to perfect the model by using actual data from more regions, and integrate the system into the emergency response platform.

ACKNOWLEDGMENTS

The current work is carried out as part of a research project supported by the National Key R&D Program of China [2018YFC0807000]. We appreciate the editor and anonymous reviewers for their constructive comments.

REFERENCES

Niu C. X. (2017) Study on the Effect of Seasonal Frozen Soil Thawing on Snowmelt Flood, Master. diss., College of Resource and Environment Sciences, Xinjiang University, Xinjiang, China.

Deutscher, and Osterreichischer A. (1900) Zeitschrift des Deutschen und oesterreichischen Alpenvereins, Reading, Mass.: Der Verein,.

Marinec, J.; Rango, A. (1986). Parameter values for snowmelt runoff modeling, *Journal of Hydrology*, 84, 197-219.

Lang, H. (1968). Relations between glacier runoff and meteorological factors observed on and outside the glacier, *IAHSPubl*, 79, 429-439.

Valeo, C.; Ho, C. L. I.; (2004). Modelling urban snowmelt runoff, *Journal of Hydrology*, 299, 3, 237-251.

Nagler, T.; Rott, H.; and Malcher, P.; et al. (2008). Assimilation of meteorogical and remote sensing data for snowmelt runoff forecasing, *Remote sensing of environment*, 112, 4, 1408-1420.

Bathurst, J. C.; Iroume, A.; and Cisneros, F.; et al. (2011). Forest impact on floods due to extreme rainfall and snowmelt in four Latin American environments 1: Field data analysis, *Journal of Hydrology*, 400, 3, 281-291.

Jost, G.; Moore, R. D.; and Smith, R.; et al. (2012). Distributed temperature-index snowmelt modelling for forested catchments, *Journal of Hydrology*, 420, 87-101.

Wigmosta, M.S., Vail, L.W., Lettenmaier, D.P., 1994. A distributed hydrology vegetation model for complex terrain. *Water Resources Research.* 30, 6, 1665–1679.

Link, T., Marks, D., Hardy, J., Albert, M., Marsh, P., 1999. Distributed simulation of snowcover mass- and energy-balance in the boreal forest. *Hydrological Processes*, 13, 2439–2452.

Shen, Y. J.; Shen, Y.; and Fink, M.; et al. (2018) Trends and variability in streamflow and snowmelt runoff timing in the southern Tianshan Mountains, *Journal of Hydrology*, 557, 173-181.

Xiong, L. H.; Guo, S. L. (2004) *Distributed Watershed Hydrological Model*. Reading, Mass.: Addison-Wesley.

Alfred T.C. Chang. (2000) Algorithm Theoretical Basis Document (ATBD) for the AMSR-E Snow Water Equivalent Algorithm, NASA, 9-14.

Lv, Y. C.; et al. (2018) Snow Estimation in the Huai River Based on Modis, *Geographical Science Research*, 7, 3, 251-257.

Wang, X. et al. (2014) Quality Control of Temperature Observation Data with Improved IDW Algorithm, *Meteorological Science and Technology*, 8, 42, 605-611.

Fang, S. F.; et al. (2008) Study on the Distribution Snowmelt Runoff Process Based on RS and GIS, *Journal of Remote Sensing*, 12, 04, 655-662.

Song, X. Y.; et al. (2012) Extraction and Analysis of Hydrological Characteristics of Yanhe Watershed Based on DEM, *Agricultural Research in the Arid Areas*, 30, 4, 200-206.

Manning R.; Griffith J. P.; Pigot T. F.; et al. (1890) *On the flow of water in open channels and pipes*. Reading, Mass.: Addison-Wesley.

Tian, H.; et al. (2011) The Possible Weather Causes for Snowmelt Flooding in Xinjiang in Mid-March 2009, *Meteorological Monthly*, 37, 5, 590-598.

Yan, Y.; et al. (2009) Establishment and Validation of Early-warning Model for Snowmelt Flood in North Xinjiang, *Arid Land Geography*, 32, 4, 552-557.